Applied Physics Letters ARTICLE pubs.aip.org/aip/apl

Optical transitions between entangled electron–phonon states in silicon

Cite as: Appl. Phys. Lett. **127**, 141102 (2025); doi: 10.1063/5.0288893
Submitted: 3 July 2025 · Accepted: 21 September 2025 ·
Published Online: 8 October 2025

Yael Gutiérrez,[1,a] Mateusz Rebarz,[2] Christoph Cobet,[3,4] Josef Resl,[4] Saúl Vázquez-Miranda,[2] Shirly Espinoza,[2] and Kurt Hingerl[4,a]

AFFILIATIONS

[1]Departamento de Física Aplicada, Universidad de Cantabria, Avenida de los Castros, s/n, 39005 Santander, Spain
[2]ELI Beamlines Facility, The Extreme Light Infrastructure ERIC, Za Radnicí 835, 25241 Dolní Brezany, Czech Republic
[3]Linz School of Education, University Linz, Altenbergerstrasse 69, A-4040 Linz, Austria
[4]Center for Surface and Nanoanalytics, University Linz, Altenbergerstrasse 69, A-4040 Linz, Austria

Note: This paper is part of the Special Topic on Advances in Spectroscopic Ellipsometry Methods and Materials Characterization.
[a]**Author to whom correspondence should be addressed:** gvelay@unican.es and kurt.hingerl@jku.at

ABSTRACT

Silicon crystallizes in the diamond structure with two atoms per unit cell and supports three optical phonon modes. However, due to the centrosymmetric nature of the lattice, these modes do not induce a net dipole moment and are therefore inactive in infrared absorption. Even in polar semiconductors, where optical phonons can be IR-active, conventional techniques such as infrared absorption and Raman spectroscopy are restricted to probing phonons at the Brillouin zone center (Γ-point). In this work, we demonstrate that time- and spectrally resolved pump–probe ellipsometry enables access to the coherent response of electron–phonon coupled states involving both valence and conduction bands. Following two-photon absorption induced by the femtosecond pump pulse, the electronic excitation relaxes and drives the generation of coherent longitudinal optical phonons along the X-direction of the Brillouin zone, followed by optical transitions of entangled electron–phonon states along the Λ-direction. This process results in a transient, strongly correlated electron–phonon state that persists for up to ≈ 300 fs. Within this coherent time window, the silicon crystal exhibits optical resonances at electronic transition energies modulated by quantized phonon contributions. Finally, we detect further sidebands in the ellipsometric spectrum, which are 81 meV apart and assign these to two-phonon-assisted electronic transitions.

Understanding ultrafast phenomena in semiconductors is pivotal for advancing materials science, offering both fundamental insights and enabling next-generation technological advancements. The investigation of ultrafast dynamics can reveal crucial information about the lifetime of excitations, the existence and evolution of entangled states, and the presence of mechanisms governing scattering processes.[1] Pump–probe techniques have become essential tools in this field, enabling the study of ultrafast dynamics with femtosecond (fs) temporal resolution. By using ultrashort laser pump pulses to excite the material, and a weaker probe beam to monitor its response at controlled time delays, these techniques allow for precise temporal tracking of changes in the probe signal to uncover the evolution and decay of generated excitations.

Time-resolved pump–probe spectroscopic ellipsometry (TRSE) has recently advanced this approach by enabling precise measurements of the real and imaginary parts of nonequilibrium, temporally varying dielectric response functions,[2] facilitating the study of ultrafast electron and lattice dynamics in various semiconductors.[3–6]

Previous TRSE measurements on semiconductors, including those on Si,[6] have used pump pulses (PPs) with photon energies above the semiconductor bandgap to study electron dynamics. This approach causes a significant deviation from equilibrium, with electronic transitions from the valence band (VB) to the conduction band (CB) generating high carrier concentrations. The resulting large number of optically excited carriers in the CB, occurring on femto- to picosecond timescales, induces various effects such as Burstein–Moss shift[3,4,7] and bandgap renormalization[3–5,8] as well as, in indirect semiconductors, bleaching of electronic transitions. Additionally, these phenomena give rise to pronounced thermalization processes that dominate the TRSE

signals, often obscuring more subtle dynamics related to electron–phonon interactions.

This work focuses on employing TRSE to probe electron–phonon interactions in Si, particularly focusing on the optical phonons, which are traditionally inaccessible via conventional optical techniques due to centrosymmetric diamond structure of Si. However, our findings demonstrate that TRSE, as an absorption-based technique, enables detection of measurable optical phonon responses in diamond-structured materials at both the Brillouin zone center and edge.

To achieve this, and in contrast to previous studies, we employed pump pulses with photon energies below or very close to the indirect bandgap of Si (i.e., 1.24 eV at room temperature). This deliberate choice of pump photon energy facilitates sub-bandgap excitation via two-photon absorption (TPA), allowing for a more controlled analysis of phonon-induced changes within the material while mitigating thermalization effects and minimizing the generation of deformation potential effects, which often dominate in single-photon absorption regimes. Notably, longitudinal optical (LO) phonon generation in Si via deformation potential has been directly observed in ultrafast pump–probe reflectivity experiments in the seminal work by Hase *et al.*[9,10] Their study highlights how, under above-bandgap excitation, electronic excitation couples to the lattice through the deformation potential, launching coherent LO phonons. In contrast, our approach via TPA provides a non-resonant pathway to examine optical phonon signatures with reduced lattice perturbation. Importantly, this approach still generates ballistic electrons and holes.[11]

We performed TRSE experiments at room temperature employing 50 fs pump pulses (PPs) with photon energies of 1.27 eV (970 nm), 1.18 eV (1050 nm), 1.08 eV (1150 nm), and 0.95 eV (1300 nm), carefully selected to lie near or below the indirect bandgap of Si. Additional technical details on the TRSE setup and the specific measurement conditions used in this work are provided in supplementary material Note 1. Transient broadband optical responses were recorded in the 1.9–3.8 eV range for time delays ranging from 50 fs to 4.5 ns. From these measurements, we extract the time-dependent complex pseudo-dielectric function $\langle\epsilon\rangle = \langle\epsilon_1\rangle + i\langle\epsilon_2\rangle$. Figure 1 shows $\Delta\langle\epsilon_1\rangle$ and $\Delta\langle\epsilon_2\rangle$ for a sub-bandgap PP photon energy of 1.08 eV. $\Delta\langle\epsilon\rangle$ for other studied sub-bandgap PP energies (i.e., 0.95, 1.18, and 1.27 eV) is shown in Fig. S2. It should be noted that we did not conduct a systematic study varying the pump photon energy and fluence to determine the optimal conditions for observing the electron–phonon coupled states discussed in this manuscript. Instead, our focus was on demonstrating the existence and characteristics of these states under selected sub-bandgap excitation conditions.

The absence of signal at twice or three times the PP photon energy indicates the lack of instantaneous second or third harmonic generation or instantaneous Raman response during the excitation process. The changes induced by the PP manifest across a broad spectral range, even far above the PP energy. Two distinct transient spectral line shapes can be clearly distinguished in the experimental $\Delta\langle\epsilon_1\rangle$ and $\Delta\langle\epsilon_2\rangle$ spectra. In this work, we focus on the periodic sidebands with an energy spacing of 57 ± 9 meV, most prominently observed between 2.8 and 3.4 eV at a delay of 100 fs after excitation. As discussed in detail below, these sidebands arise from the coupling of LO phonons to the optical transitions, and we refer to them as longitudinal optical phonon sidebands (LOPSs). Notably, a second set of features, characterized by an energy spacing of approximately 81 ± 7 meV, are visible between 2.2 and 2.6 eV. They are attributed to two-phonon processes and will be referred to as two-phonon sidebands (TPSs) and are briefly addressed for completeness although they are not the primary focus of this work.

Although the LOPSs are discernible in both $\Delta\langle\epsilon_1\rangle$ and $\Delta\langle\epsilon_2\rangle$ spectra, only $\Delta\langle\epsilon_1\rangle$ for the pump–probe configuration with a photon energy of 1.08 eV is shown in Fig. 2, as it offers better contrast for illustrating the spectral evolution at different time delays. Figure 2(a) shows the change in the real part of the pseudo-dielectric function $\Delta\langle\epsilon_1\rangle$ at selected time delays. The curves are vertically offset for clarity. A clear modification of the pseudo-dielectric function induced by the PP is observed.

The spectral oscillations displayed in Fig. 2(c), with a periodicity of 57 ± 9 meV in the 2.8–3.4 eV range, correspond to the LOPSs. These oscillations do not appear immediately but begin to emerge shortly after excitation, reaching their maximum amplitude around 100 fs, as depicted in Fig. 2(e). The periodic structures gradually decay and are no longer visible after approximately 300 fs.

This behavior contrasts with the results reported by Hase *et al.*,[9,10] where coherent LO phonons were observed as oscillations in the time domain using single wavelength transient reflectivity measurements, with a dephasing time of approximately 3 ps. These single wavelength reflectivity changes are due to an in-plane anisotropic and

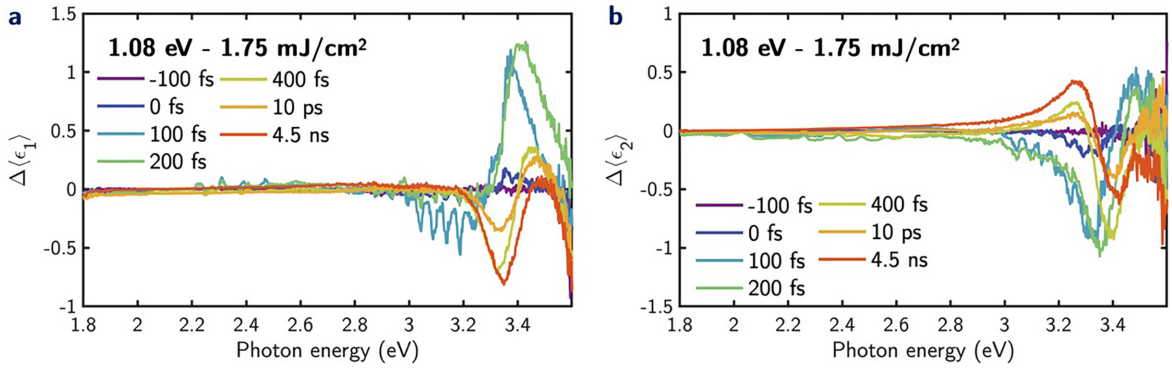

FIG. 1. Transient real and imaginary parts of the pseudo-dielectric function (a) $\Delta\langle\epsilon_1\rangle$ and (b) $\Delta\langle\epsilon_2\rangle$ at different time delays for a PP photon energy of 1.08 eV and a fluence of 1.75 mJ/cm^2.

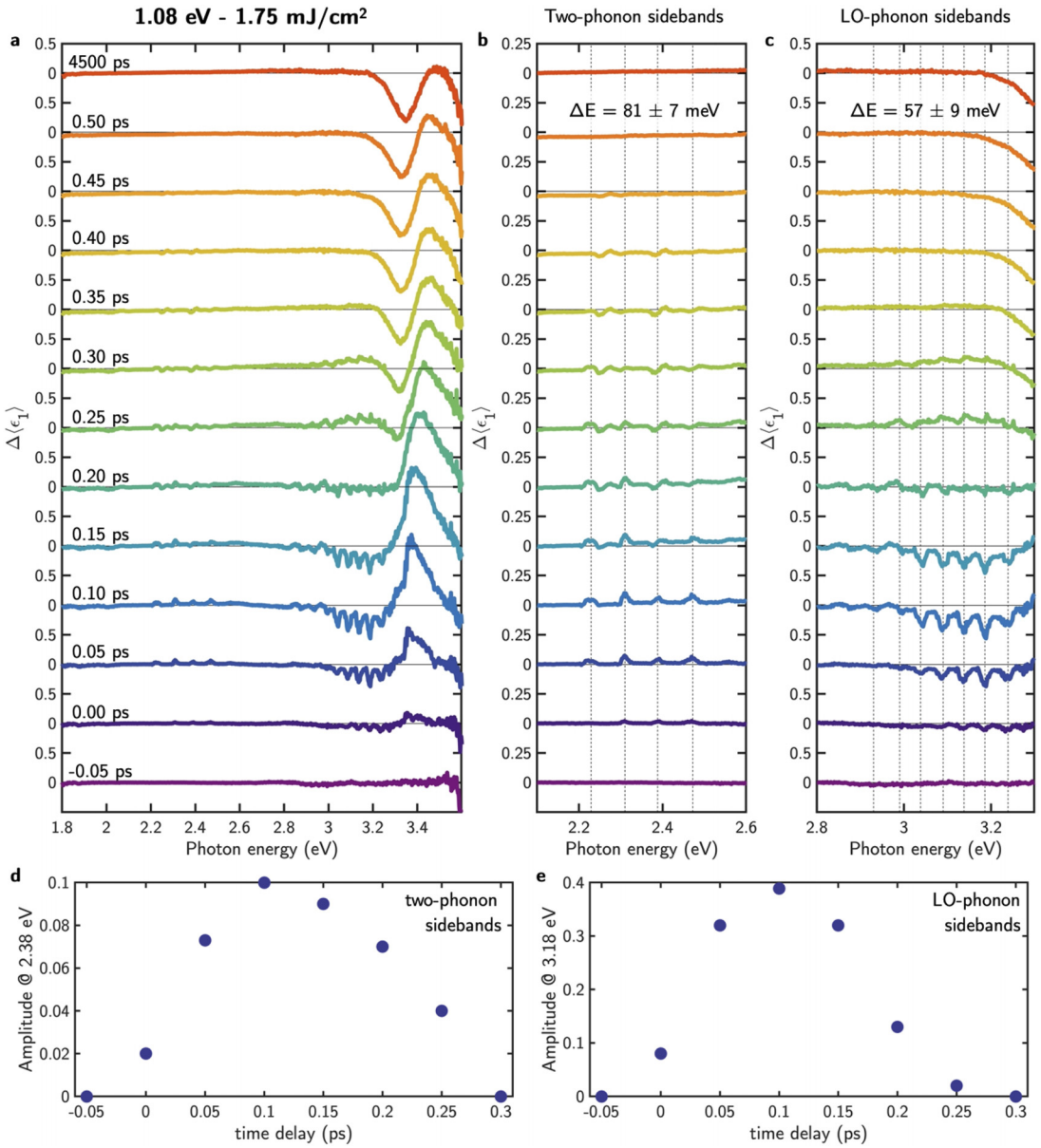

FIG. 2. (a) Change in the real part of the pseudo-dielectric function $\Delta\langle\epsilon_1\rangle$ at different time delays, with curves vertically shifted for clarity. The photon energy of the pump is 1.08 eV, and its fluence is 1.75 mJ/cm^2. (b) Two-phonon sidebands (TPS): Oscillations with a periodicity of 81 ± 7 meV in the range of 2.1–2.6 eV. (c) Longitudinal optical phonon sidebands (LOPS): Oscillations with a periodicity of 57 ± 9 meV in the range of 2.8–3.4 eV. Evolution in time of the amplitude of (d) the two-phonon sidebands measured at 2.38 eV and (e) the longitudinal optical phonon sidebands measured at 3.18 eV.

macroscopic strain state, which modifies the electronic transitions due to deformation potential. It should be noted that these measurements also show the entanglement between electrons and phonons (manifested as deformations) but can be explained with a macroscopic perturbation. In our case, the temporal resolution is insufficient to resolve oscillations at the LO phonon frequency of Si. Nonetheless, the LO phonon signatures in our measurements appear as clear periodic modulations in the energy domain, with a markedly shorter dephasing time of approximately 300 fs. This contrast underscores the distinct phonon generation mechanisms at play: Above-bandgap excitation in Hase's work leads to a macroscopic strain response, whereas our experiment, based on sub-bandgap two-photon absorption, triggers a microscopic, quantum-mechanical relaxation process. Figure 2(b) shows the TPS in the spectral range between 2.2 and 2.6 eV, with an energy spacing of 81 ± 7 meV, and a lifetime of 300 fs as shown in Fig. 2(d).

Before delving into the discussion of the experimental findings, it is important to clarify the types of relaxation dynamics that can be detected by TRSE and the temporal regimes that govern each stage of this process: The TRSE setup allows the spectral measurement of ultrafast changes in both the real and imaginary parts of the dielectric function, enabling the capture of different relaxation processes as the material returns to thermodynamic equilibrium. Unlike ultrafast optical diffraction setups,[1] which focus primarily on coherent effects, TRSE provides information across multiple temporal regimes, capturing both coherent and incoherent dynamics. These regimes include the coherent relaxation regime (≈200 fs), the non-thermal regime (≈2 ps), the hot excitation regime (≈100 ps), and the isothermal regime (>100 ps) (see Fig. 1.7 in Ref. 1).

The coherent regime is characterized by the appearance of strongly coupled many-particle wavefunctions in the solid. To theoretically describe this regime, it is essential to consider the off-diagonal elements of the density matrix involving electrons and phonons, which can be effectively modeled by solving the semiconductor Bloch equations.[12] In the non-thermal regime, scattering events (e.g., electron–electron interactions) dominate, causing the initially sharp energy distribution induced by the PP to smear out, thereby producing dephasing and suppressing measurable coherence and beating effects after ≈ 100 fs. In the hot excitation regime, electronic energy is primarily transferred to the lattice, leading to the decay of high-energy optical phonons into acoustic phonons. Finally, in the isothermal regime, the electrons reach thermal equilibrium with the lattice, and heat conduction takes place. When interpreting the experimental results, it is crucial to consider these distinct temporal regimes, as each governs different stages of relaxation and energy redistribution within the material.

To better understand the origin of the observed spectral features in the time-resolved $\Delta\langle\epsilon\rangle$ spectra, we now discuss the excitation mechanism triggered by the pump and the specific electronic and vibrational responses probed by the delayed probe pulse.

We begin by analyzing the pump process in detail, which is schematized in Fig. 3(a). In centrosymmetric materials like silicon, single-photon absorption typically involves dipole-allowed transitions between electronic states of opposite parity, accompanied by a change in orbital angular momentum ($\Delta l = \pm 1$). In contrast, two-photon absorption (TPA) follows different selection rules: $\Delta l = (0, \pm 2)$ and $\Delta m \neq 0$, enabling transitions between states of the same parity (even-to-even or odd-to-odd), while transitions between states of opposite parity are forbidden.[14]

In our case, the pump photon energy is below half the direct bandgap of silicon, and thus the TPA process requires phonon assistance to satisfy momentum conservation.[11] Specifically, longitudinal or transverse acoustic LA/TA phonons along the Δ-direction provide the necessary crystal momentum. These phonons are thermally populated at room temperature and belong to even irreducible representations,[15] preserving the parity selection rules of the TPA process. Consequently, the pump excitation in our experiment involves a phonon-assisted indirect transition from the VB maximum to the CB along the Δ-direction, where the two-photon process promotes an electron between states of the same parity, while the LA/TA phonon supplies the required momentum. This combined excitation mechanism is illustrated in Fig. 3(a).

Following the PP and TPA, the system enters a high-energy, non-equilibrium state, which then begins to relax. With TPA, the density of charge carriers is relatively low, making carrier–carrier scattering unlikely. Therefore, the redistribution of energy from the electronic degrees of freedom to the phononic ones is observable for 300 fs. Additionally, due to the low carrier density, Auger processes are also improbable. Thus, the primary remaining relaxation mechanism is optical phonon scattering, which is energetically the most efficient one for approaching thermodynamic equilibrium. For a PP with 1.08 eV a surplus energy for the electron–hole excitation of ∼0.92 eV remains (∼2 × 1.08 eV − 1.24 eV). As shown in the phonon dispersion of Si in Fig. 3(c), the LO phonon branch has a relatively flat dispersion along the Λ-direction, with an energy of 63 meV (15.3 THz) at the Γ-point and 52.1 meV (12.4 THz) at the L-point (p. 2561 of Ref. 16). If one electron has to transfer ≈0.92 eV of excess energy, approximately 14–18 electron–optical phonon scattering events would be required, as each LO phonon along the Λ-direction carries between 52.1 and 63 meV of energy. Such an electron–phonon cascade model, illustrated

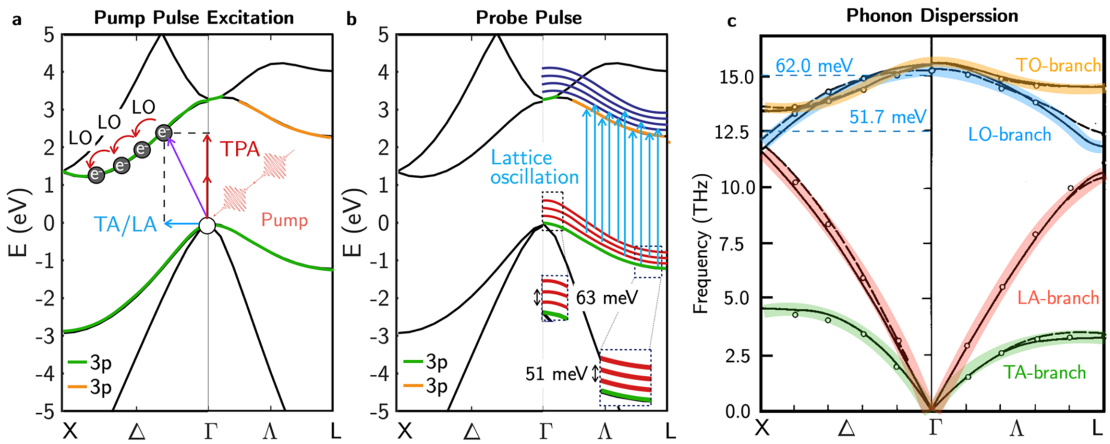

FIG. 3. (a) Scheme of the excitation mechanism triggered by the pump. (b) Scheme of the electronic and vibrational responses probed by the delayed probe pulse. (c) Phonon dispersion of Si at room temperature reproduced with permission from International Atomic Energy Agency, in *Symposium on Inelastic Scattering of Neutrons in Solids and Liquids*, Chalk River, on 10–14 September 1962 (IAEA, Vienna, 1963), pp. 3–22. Copyright 1963, International Atomic Energy Agency.[13]

in Fig. 3(a), has been proposed for inelastic light scattering in 1971 to explain experimental Raman data of higher order Stokes shifted lines.[17] Raman measurements on YbS and comparison with possible other explanations point out the importance of lifetime effects of the excited electronic state.[18]

The time-dependent dielectric response observed in Figs. 2(b) and 2(c) supports this interpretation. Notably, the phonon sidebands' signal does not appear instantaneously with the pump pulse but grows progressively, reaching a maximum around 100 fs. Since spectroscopic ellipsometry probes changes in the complex dielectric function linked to optical transitions, this delay indicates that the observed spectral features do not originate from direct phonon generation by the pump, but rather from a relaxation process after pump excitation. The gradual rise in transition amplitude is thus consistent with the generation of optical phonons as electrons and holes relax and transfer their excess energy to the lattice, highlighting the kinetic character of the carrier–phonon coupling dynamics in this low-density, nonequilibrium regime.

Consequently, the probed dipolar optical transitions in $\Delta\langle\epsilon\rangle$ between 2.8 and 3.4 eV correspond to transitions along the Λ-direction, as illustrated in Fig. 3(b). These transitions, which occur near or at the L-point between electronic states of opposite parity, do not involve the creation or annihilation of individual phonons. Instead, during the initial coherent regime, the electronic band structure is modulated by collective lattice oscillations arising from the entangled electron–nuclei system generated during the relaxation of the pump excitation. The observed longitudinal LOPSs result from optical transitions between vibrationally quantized states of the silicon lattice, superimposed on the valence and conduction electronic bands. This interaction manifests as "sidebands," i.e., copies of the original band structure shifted in energy by integer multiples of the LO phonon energy. The measured energetic spacing between these sidebands in Fig. 2(b) is approximately 57 ± 9 meV, consistent with the LO phonon energy near the L-point as shown in Fig. 3(c). This observation further suggests that the optical transitions contributing to the LOPS extend away from the L-point along the Λ-direction in the Brillouin zone. Such an extension may result from intervalley scattering processes and/or the involvement of a superposition of phonons along the Λ-directions. Specifically, phonons with momenta along Λ-directions, i.e., $\langle 1,0,0\rangle$, $\langle 0,1,0\rangle$, and $\langle 0,0,1\rangle$, can combine linearly to yield an effective momentum transfer toward the L-point at $\langle 1,1,1\rangle$.

Lax and Burstein[19] have discussed the coupling between electronic and nuclear motion. They demonstrated that the transition from the initial Born–Oppenheimer state, characterized by a product wavefunction for electrons (φ) and nuclei (X), described as $\psi_i(\vec{r},\vec{x}) = \varphi_a(\vec{r},\vec{x})\,X_{am}(\vec{x})$, to a final state $\psi_f(\vec{r},\vec{x}) = \varphi_b(\vec{r},\vec{x})\,X_{bm}(\vec{x})$, involves energy conservation for the nuclear transition energies $\delta(E_n - E_m - \hbar\omega)$. When considering coupled electronic–phononic transitions involving oscillating nuclei, energy conservation can thus be represented as $\delta((E_i - E_f) \pm (E_n - E_m) - \hbar\omega)$, where E_i, (E_f) is the initial (final) electronic energy, and E_n and E_m are the quantized energy levels corresponding to phonons. The zeros of the δ function correspond to critical points for the oscillating nuclei system and provide measurable resonances in absorption. The structure of the transitions mimics the Franck–Condon effect in molecules which describes the overlay of electronic and vibrational transitions in molecules. This concept has also been extended to explain similar phenomena in color centers or defects in solids.[20] Because the CB and VB along the Λ-direction are parallel, similar to discrete electronic energies of molecules, the calculation of the transition matrix elements and selection rules can proceed in the same way, as explained in Chap. 16.4 and 16.5 of Ref. 21.

This phenomenon has already been reported in the literature by using time-resolved diffraction techniques, which directly map the breathing motion, i.e., nuclei oscillations, of the crystal. Time-resolved electron diffraction experiments on germanium,[22] nickel,[23] and the 2D material WSe_2[24] have reported the emission and occupation of zone boundary phonons during electron relaxation processes. These published results obtain phonon state lifetimes of >100 ps and phonon buildup times of ≈ 5 ps, in contrast with the ≈ 100 fs observed in the experiments reported here. However, the electronic relaxation process through LO phonons has never been observed through optical means before. In conclusion, while electron diffraction experiments offer valuable insights into lattice oscillation lifetimes and structural deformations, such as the work by Hase *et al.*[9,10] using above-bandgap excitation to probe coherent LO phonons originating from a deformation potential, the TRSE measurements presented here access a different regime, probing the lifetime of a coherent many-body wavefunction involving coupled electron–phonon states. To avoid ambiguity, we provide a detailed explanation of this concept in supplementary material Note 3, where we clarify that the terms "coherent wavefunction" and "entangled state" refer to the same underlying physical phenomenon.

Finally, we briefly discuss the origin of the TPS. These transitions occur along the Δ-direction of the Brillouin zone, where silicon indirect bandgap minimum is located. The 81 meV energy spacing is attributed to a combination of a 63 meV LO(Γ) phonon and an 18.2 meV TA(X) phonon. These replicas indicate coherent oscillations of Si atoms at both LO and TA phonon frequencies. The associated optical transitions occur near the X point but have weaker intensity than the LO phonon sidebands due to less favorable electronic band alignment and broader energy averaging.

The presence of TA phonons reflects LO phonon relaxation processes, which predominantly proceed via decay into TA and LA phonons at the Brillouin zone edge, consistent with theoretical *ab initio* predictions.[25] Unlike the LOPS features, these two-phonon transitions cannot be described using the electron–phonon cascade model, as the TA phonon provides momentum, altering selection rules. A full theoretical treatment likely requires diagrammatic methods to properly account for the coupled electron–phonon–photon dynamics.

As a final point, we discuss the tilted-S-shaped feature observed between 3.2 and 3.5 eV, which exhibits a lifetime exceeding 4.5 ns (upper time limit of our setup). We hypothesize that this feature arises from charge separation in k-space. Specifically, the electron is likely trapped, potentially for several milliseconds, in one of the six conduction band minima of silicon, while the hole remains at the valence band maximum, forming an electron–hole pair. This spatial separation in momentum space can result in an excited state with a lifetime extending up to the millisecond range in silicon.

To conclude, in this work, we demonstrate that a time- and spectrally resolved spectroscopic ellipsometry setup can provide fresh perspectives on the quantum mechanical interactions between electrons and nuclei in silicon. For approximately a quarter of a picosecond, electrons and nuclei exhibit coherent oscillations, governed by the

quantized frequencies and energies of the nuclear motion. These nuclear quantization energies overlay the electronic energy levels, manifesting as "parallel" phonon bands superimposed to the purely electronic ones. In absorption measurements, this results in LO phonon sidebands along the Λ-direction and combined LO+TA two-phonon sidebands along the Δ-direction. These observations indicate the potential to probe complex 2- or 3-(quasi-)particle eigenstates.

See the supplementary material for supplementary Note 1, which provides a description of the experimental setup and measurement conditions, and supplementary Note 2, which presents the transient pseudo-dielectric function for different pump photon energies: 0.98 eV and 1.00 mJ/cm^2, 1.08 eV and 1.75 mJ/cm^2, 1.18 eV and 0.63 mJ/cm^2, and 1.27 eV and 0.97 mJ/cm^2.

The authors thank Dr. Maria Losurdo for her motivating role in this work and for laying its cornerstones during the early investigations, when measurements on thin GaS layers yielded surprising and initially unclear results. Furthermore, the support of the ELI group leader Jakob Andreasson is highly acknowledged. We further thank the ELI Beamlines facility in Dolní Břežany, Czech Republic, for providing beamtime and thank the instrument group and facility staff for their assistance. Funding for the Linz group was provided by the project LIT-2021-10-SEED-114. Y.G. acknowledges funding from a Ramon y Cajal Fellowship (RYC2022-037828-I). M.R., S.V-M, and S.E. were supported by the project ADONIS (No. CZ.02.1.01/0.0/0.0/16-019/0000789).

AUTHOR DECLARATIONS

Conflict of Interest

The authors have no conflicts to disclose.

Author Contributions

Yael Gutierrez: Conceptualization (equal); Data curation (equal); Funding acquisition (equal); Investigation (equal); Methodology (equal); Project administration (equal); Supervision (equal); Visualization (equal); Writing – original draft (equal); Writing – review & editing (equal). **Mateusz Rebarz:** Investigation (equal); Methodology (equal). **Christoph Cobet:** Investigation (equal); Methodology (equal). **Josef Resl:** Investigation (equal); Visualization (equal). **Saul Vazquez-Miranda:** Investigation (equal); Methodology (equal); Visualization (equal). **Shirly Espinoza:** Investigation (equal); Methodology (equal); Project administration (equal); Supervision (equal); Writing – original draft (equal); Writing – review & editing (equal). **Kurt Hingerl:** Conceptualization (equal); Funding acquisition (equal); Investigation (equal); Methodology (equal); Project administration (equal); Supervision (equal); Writing – original draft (equal); Writing – review & editing (equal).

DATA AVAILABILITY

The data underlying this study are openly available in Zenodo at https://zenodo.org/records/13939334 (Ref. 26).

REFERENCES

[1]J. Shah, *Ultrafast Spectroscopy of Semiconductors and Semiconductor Nanostructures* (Springer, Berlin, Heidelberg, 1999).
[2]S. Richter, O. Herrfurth, S. Espinoza, M. Rebarz, M. Kloz, J. A. Leveillee, A. Schleife, S. Zollner, M. Grundmann, J. Andreasson, and R. Schmidt-Grund, New J. Phys. **22**, 083066 (2020).
[3]E. Baron, R. Goldhahn, S. Espinoza, M. Zahradník, M. Rebarz, J. Andreasson, M. Deppe, D. J. As, and M. Feneberg, J. Appl. Phys. **134**, 075702 (2023).
[4]E. Baron, R. Goldhahn, S. Espinoza, M. Zahradník, M. Rebarz, J. Andreasson, M. Deppe, D. J. As, and M. Feneberg, J. Appl. Phys. **134**, 075703 (2023).
[5]C. Emminger, S. Espinoza, S. Richter, M. Rebarz, O. Herrfurth, M. Zahradník, R. Schmidt-Grund, J. Andreasson, and S. Zollner, Phys. Status Solidi RRL **16**, 220005 (2022).
[6]S. Espinoza, S. Richter, M. Rebarz, O. Herrfurth, R. Schmidt-Grund, J. Andreasson, and S. Zollner, Appl. Phys. Lett. **115**, 052105 (2019).
[7]E. Burstein, Phys. Rev. **93**, 632 (1954).
[8]K.-F. Berggren and B. E. Sernelius, Phys. Rev. B **24**, 1971 (1981).
[9]M. Hase, M. Kitajima, A. M. Constantinescu, and H. Petek, Nature **426**, 51 (2003).
[10]M. Hase, M. Katsuragawa, A. M. Constantinescu, and H. Petek, New J. Phys. **15**, 055018 (2013).
[11]M. Spasenović, M. Betz, L. Costa, and H. M. van Driel, Phys. Rev. B **77**, 085201 (2008).
[12]T. Meier, P. Thomas, and S. W. Koch, in *Ultrafast Phenomena in Semiconductors* (Springer, New York, NY, 2001), pp. 1–92.
[13]G. Dolling, "Lattice vibrations in crystals with the diamond structure," in *Symposium on Inelastic Scattering of Neutrons in Solids and Liquids, Chalk River, ON, 10–14 September 1962* (IAEA, Vienna, 1963), pp. 37–48.
[14]K. D. Bonin and T. J. McIlrath, J. Opt. Soc. Am. B **1**, 52 (1984).
[15]P. Y. Yu and M. Cardona, *Fundamentals of Semiconductors* (Springer, Berlin, Heidelberg, 2010).
[16]O. Madelung, U. Rössler, and M. Schulz, *Group IV Elements, IV-IV and III-V Compounds. Part B - Electronic, Transport, Optical and Other Properties* (Springer-Verlag, Berlin/Heidelberg, 2002).
[17]R. M. Martin and C. M. Varma, Phys. Rev. Lett. **26**, 1241 (1971).
[18]R. Merlin, G. Güntherodt, R. Humphreys, M. Cardona, R. Suryanarayanan, and F. Holtzberg, Phys. Rev. B **17**, 4951 (1978).
[19]M. Lax and E. Burstein, Phys. Rev. **97**, 39 (1955).
[20]M. Lax, J. Chem. Phys. **20**, 1752 (1952).
[21]H. Haken and H. C. Wolf, *Molekülphysik und Quantenchemie* (Springer-Verlag, Berlin/Heidelberg, 2006).
[22]F. Murphy-Armando, É. D. Murray, I. Savić, M. Trigo, D. A. Reis, and S. Fahy, Appl. Phys. Lett. **122**, 012202 (2023).
[23]P. Maldonado, T. Chase, A. H. Reid, X. Shen, R. K. Li, K. Carva, T. Payer, M. Horn von Hoegen, K. Sokolowski-Tinten, X. J. Wang, P. M. Oppeneer, and H. A. Dürr, Phys. Rev. B **101**, 100302 (2020).
[24]L. Waldecker, R. Bertoni, H. Hübener, T. Brumme, T. Vasileiadis, D. Zahn, A. Rubio, and R. Ernstorfer, Phys. Rev. Lett. **119**, 036803 (2017).
[25]A. Debernardi, S. Baroni, and E. Molinari, Phys. Rev. Lett. **75**, 1819 (1995).
[26]Y. Gutierrez, M. Rebarz, C. Cobet, J. Resl, M. Graml, S. Vazquez-Miranda, S. Espinoza, and K. Hingerl (2024). "Silicon time-resolved pump-probe spectroscopic ellipsometry data files," Zenodo. https://doi.org/10.5281/zenodo.13939334